Supplementary materials

Disparate evolution mechanisms and optical absorption for transboundary soot particles passing through inland and sea pathways

Jian Zhang[1], Zexuan Zhang[2], Keliang Li[2], Xiyao Chen[2], Xinpeng Xu[2], Yangmei Zhang[3], Anzhou Han[4], Yuanyuan Wang[5], Jing Ding[1], Liang Xu[6], Yinxiao Zhang[7], Hongya Niu[8], Shoujuan Shu[2], and Weijun Li[2,*]

[1]School of Environmental and Material Engineering, Yantai University, Yantai 264005, China

[2]Key Laboratory of Geoscience Big Data and Deep Resource of Zhejiang Province, Department of Atmospheric Sciences, School of Earth Sciences, Zhejiang University, Hangzhou 310027, China

[3]Key Laboratory of Atmospheric Chemistry, China Meteorological Administration, Beijing 100081, China

[4]Trier College of Sustainable Technology, Yantai University, Yantai 264005, China

[5]Hangzhou International Innovation Institute of Beihang University, Hangzhou 310000, China

[6]College of Sciences, China Jiliang University, Hangzhou 310018, China

[7]Flight College, Shandong University of Aeronautics, Binzhou 256600, China

[8]Key Laboratory of Resource Exploration Research of Hebei Province, Hebei University of Engineering, Handan 056038, China

[*]Corresponding Email: liweijun@zju.edu.cn (W. J. Li)

Text S1. The classification of individual particles

Based on morphology and elemental compositions of particles, six basic types of aerosol components were classified as soot, mineral, S-rich, organic matter (OM), metal, and fly ash.

Soot particles are aggregation of many carbonaceous spheres (Figure 3a) and mainly contain C and minor O. Mineral particles mainly contain O, Si, and Al elements and present irregular shapes. S-rich particles, also called secondary inorganic aerosols, are mainly comprised of S, O, and N elements and generally are the mixtures of $(NH_4)_2SO_4$ and NH_4NO_3 (Li et al., 2016). OM particles mainly contain C, O, and Si and often exhibit near-spherical morphology or appear as coatings on S-rich particles. Metal and fly ash particles are mainly composed of O, Si, and metallic elements (e.g., Al and Fe) and present the morphology of single sphere or aggregation of several spheres.

Because we mainly focused on soot particles, individual particles were further classified into soot-containing, S-OM/metal/fly ash/mineral, S-rich, and OM/metal/fly ash/mineral particles based on their mixing states.

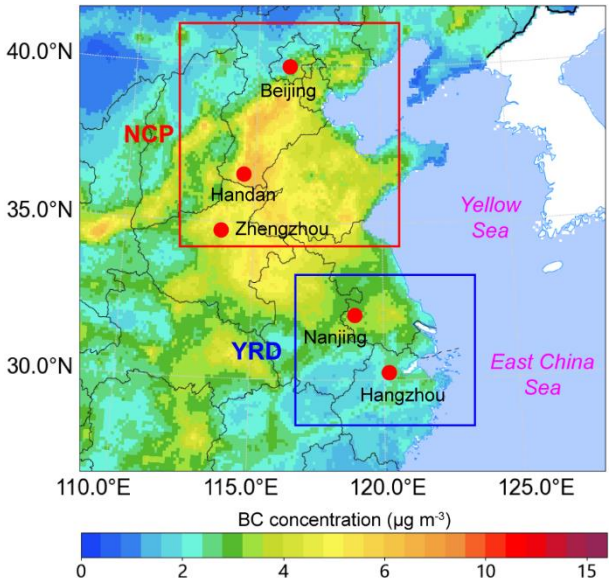

Figure S1. Spatial distribution of monthly averaged black carbon (BC) surface concentration in eastern China during December 2017 with the location of observation sites in the North China Plain (NCP) and the Yangtze River Delta (YRD) (http://tapdata.org.cn).

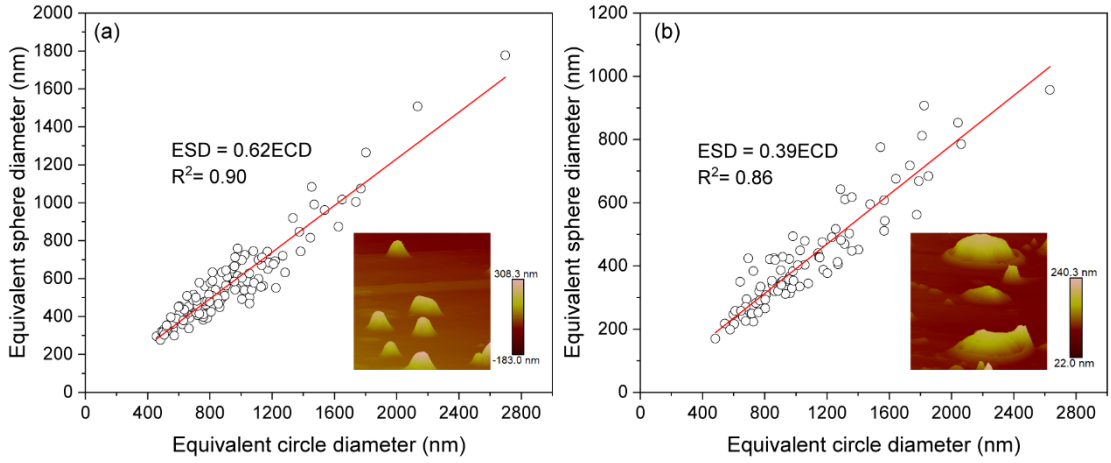

Figure S2. Linear correlation between the equivalent circle diameter (ECD) and the equivalent sphere diameter (ESD) of haze particles during two transboundary transport events. (a) Haze particles transported through the inland pathway. (b) Haze particles transported through the sea pathway. Typical atomic force microscopy (AFM) images of transported haze particles are displayed in the lower right corner in panels (a) and (b).

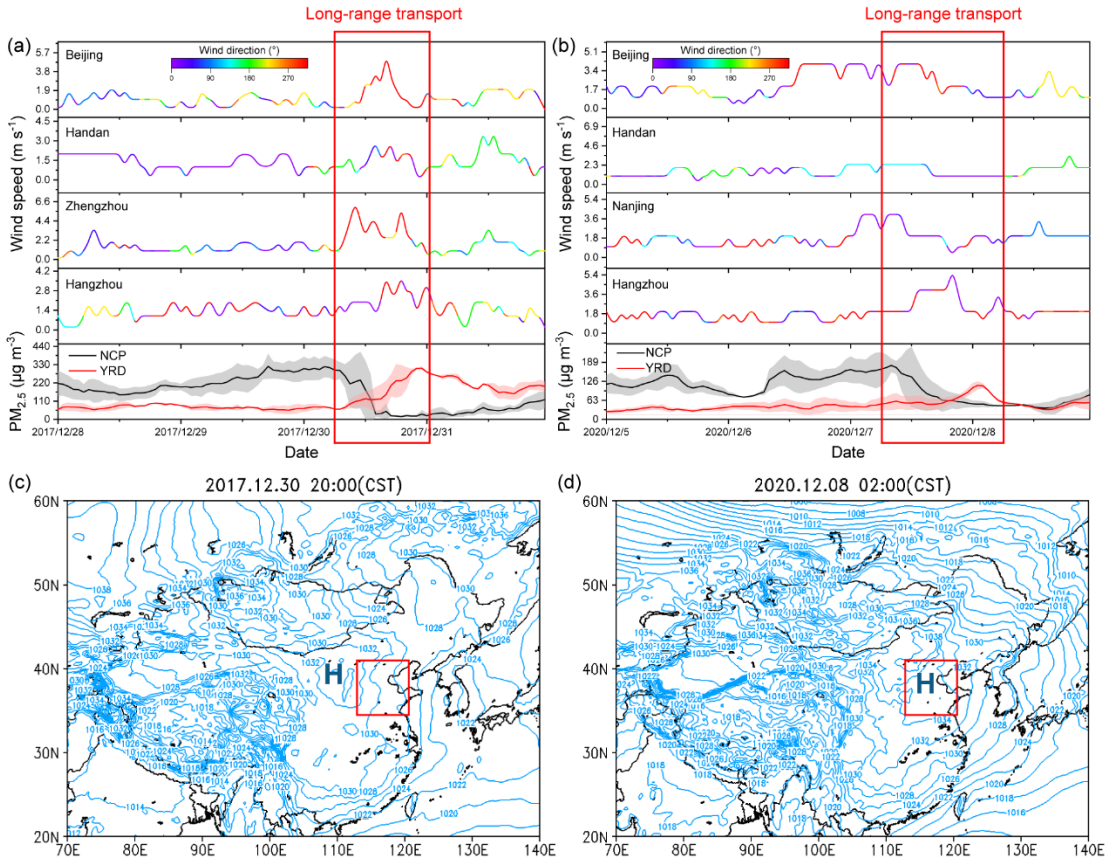

Figure S3. Time series of winds and $PM_{2.5}$ concentrations at different observation sites and sea level pressure distribution in China. (a) Winds and $PM_{2.5}$ concentrations during December 28-31, 2017. (b) Winds and $PM_{2.5}$ concentrations during December 5-8, 2020. (c) Sea level pressure distribution at 20:00 (local time) on December 30, 2017. (d) Sea level pressure distribution at 2:00 on December 8, 2020. Red rectangular boxes in panels (c) and (d) represent the NCP. CST is China local standard time; H is high pressure.

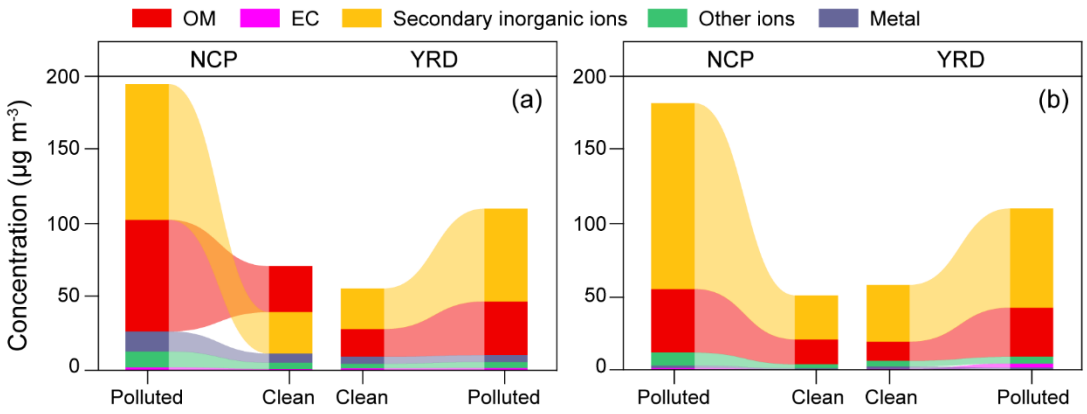

Figure S4. Variations in chemical compositions in $PM_{2.5}$ in the NCP and the YRD during two transboundary transport events. (a) Transportation through the inland pathway. (b) Transportation through the sea pathway.

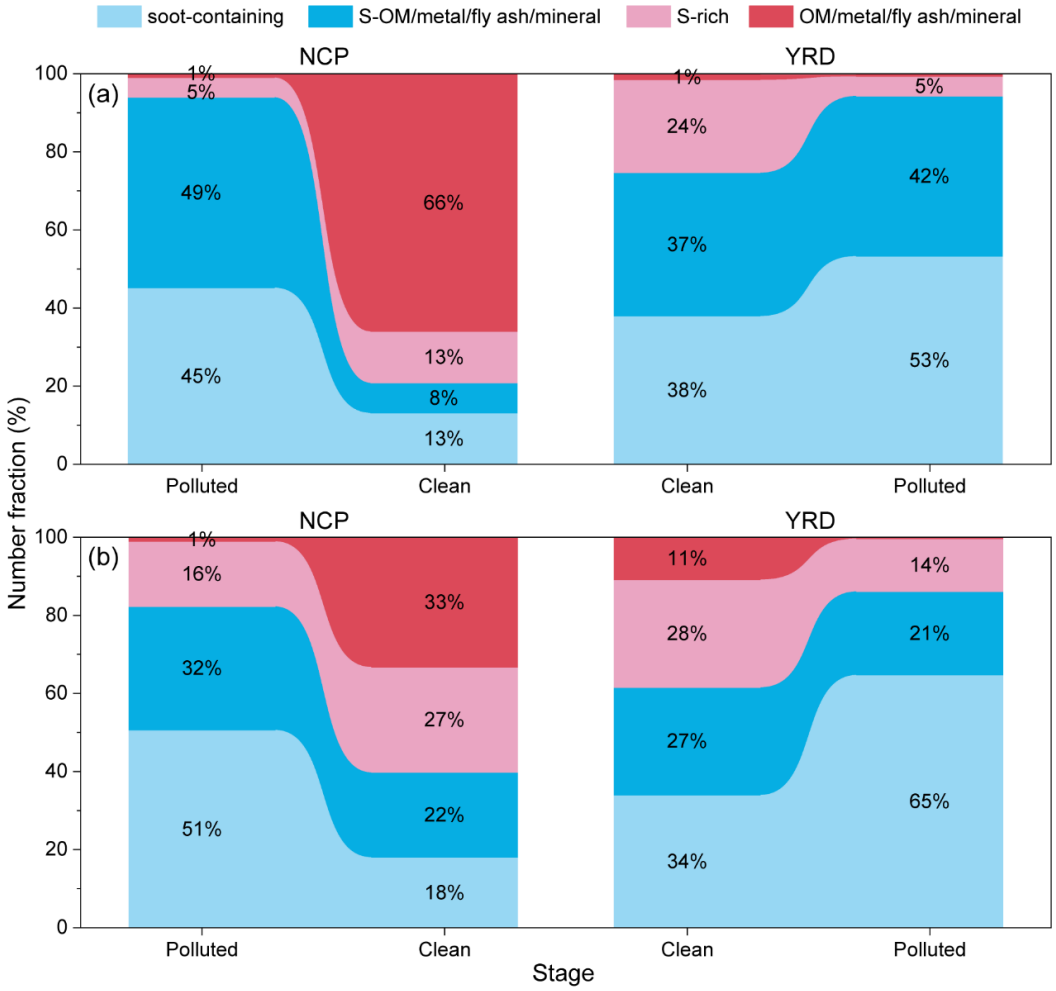

Figure S5. Variations in number fractions of individual particles in the NCP and the YRD during two transboundary transport events. (a) Transportation through the inland pathway. (b) Transportation through the sea pathway.

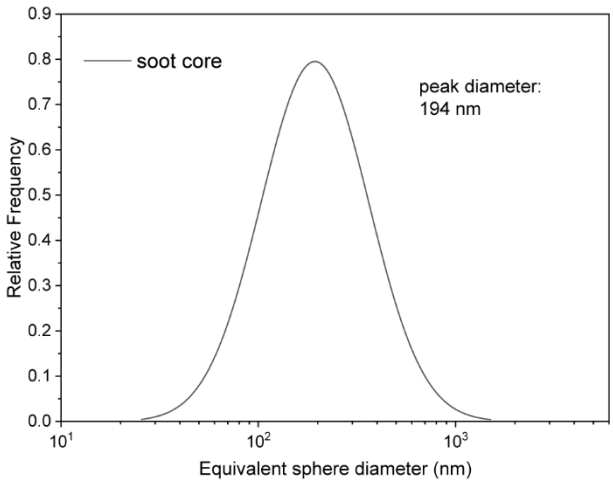

Figure S6. Size distribution of soot cores in individual soot-containing particles.

Table S1. The average relative humidity (RH) in the YRD when haze pollutants were transported from the NCP into the YRD through the inland and the sea pathways.

Transport pathway	Average RH
Inland	83%
Sea	90%

Table S2. The change in absorption enhancement simulated by core-shell Mie theory per unit the change in core-shell size ratio ($\Delta E_{abs}/\Delta(D_p/D_c)$) of soot-containing particles during the transboundary transport through the inland and the sea pathways.

Transport pathway	$\Delta E_{abs}/\Delta(D_p/D_c)$
Inland	0.01
Sea	0.03

Supplementary references

Li, W., Sun, J., Xu, L., Shi, Z., Riemer, N., Sun, Y., Fu, P., Zhang, J., Lin, Y., Wang, X., Shao, L., Chen, J., Zhang, X., Wang, Z., and Wang, W.: A conceptual framework for mixing structures in individual aerosol particles, J. Geophys. Res.-Atmos., 121, 13784-13798, https://doi.org/10.1002/2016JD025252, 2016.